Dose Rate Distribution in Triple-Layered Dielectric Cylinder with Irregular Cross Section Irradiated by Plane Wave Sources*

Henry S. Ho†

ABSTRACT

Previous investigations have shown that absorptions of microwave energy in biological bodies depend, in part, on the size and shape of the biological bodies. Calculations of dose rate distributions in regularly-shaped biological tissues have been reported. In this investigation, dose distributions are calculated for a human thigh simulated by a dielectric cylinder with irregular cross section. Method of moments is used in the investigation. The results indicate possibility of using method of moments to calculate dose distribution in a two-dimensional irregularly-shaped biological body. It is concluded that additional research is needed to determine dose rate distribution in three-dimensional irregularly-shaped biological bodies.

Introduction

Current microwave biological effects research uses animals and cell cultures. It has been shown that the pattern of absorption of microwave energy by a biological body depends on the size, shape and composition of the body; the type of electromagnetic field to which the body is exposed; and the source frequency of the microwave energy [1, 2]. Previous models used for calculations of dose rate distribution (time rate of absorbed energy per unit mass) in biological bodies have been limited to regularly-shaped objects much as slabs [3], circular cylinders [4], and spheres [5, 6]. However, dose calculations are needed for dielectric models that simulate the geometry and composition of biological bodies. The purpose of this theoretical investigation is to determine the plane wave induced dose rate distribution in a dielectric cylinder with irregular cross section. The dielectric cylinder is assumed to be infinitely long and its triple-layered cross section remains the same along the axis of the cylinder. This rather simplistic model is used so that the formulation and calculation can be reduced to that of a two-dimensional problem. Figure 1 shows the cross section of the dielectric cylinder irradiated by an incident plane wave. The real and lossy parts of the dielectric constants used in this calculation have been reported [7] and are shown in Table 1.

* Manuscript received April 10, 1975; in revised form September 2, 1975.

† U.S. Department of Health, Education, and Welfare, Public Health Service, Food and Drug Administration, Bureau of Radiological Health, Division of Biological Effects, Rockville, Maryland 20852.

421-432

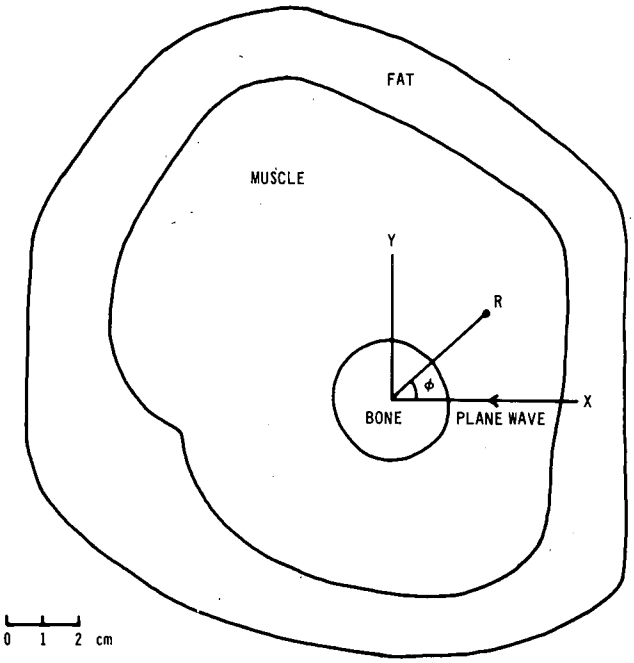

Figure 1 Thigh model simulated by a dielectric cylinder with irregular cross section.

TABLE 1
COMPLEX DIELECTRIC CONSTANTS VS. FREQUENCY

Frequency	Fat and Bone		Muscle	
MHz	$\epsilon'_{f,b}$	$\epsilon''_{f,b}$	ϵ'_m	ϵ''_m
27	20.00	10.16	108.0	377.5
433	5.61	1.96	52.8	47.4
750	5.61	1.45	51.5	30.2
918	5.61	1.31	51.4	25.2
1500	5.48	0.99	49.4	17.5
2450	5.48	0.86	47.3	16.2

$\epsilon'_{f,b}$ Real part of dielectric constant, fat and bone.
$\epsilon''_{f,b}$ Imaginary part of dielectric constant, fat and bone.
ϵ'_m Real part of dielectric constant, muscle.
ϵ''_m Imaginary part of dielectric constant, muscle.

The problem encountered in this investigation is more lengthy and complicated than the circular cylinder case. One method of solution, as reported by Yee [8], is to use the summation of cylindrical waves and to match the boundary conditions at discrete points. The cylindrical wave terms are coupled due to the irregular shape of the cross section of the dielectric cylinder. Therefore, the coefficients of all the cylindrical wave terms needed for convergence are calculated in one large set of simultaneous equations. Furthermore, the deviation of the cross section from circular shape causes the series of cylindrical waves to converge more slowly than the circular case. Hence more cylindrical wave terms are actually needed than in the circular case. Calculations for dose rate patterns due to 433 MHz to 2450 MHz plane wave sources are attempted with a

dielectric model simulating the size and shape of a section of human thigh (Figure 1). However, convergence of the sums of cylindrical waves was not attained within reasonable computation time limits.

Moment Method

Moment method as reported by Harrington [9] is particularly useful for solving electromagnetic problems dealing with irregular shaped objects. A brief summary of the method is considered in the following.

Consider a dielectric body with its complex dielectric constant as a function of position: $\epsilon(\vec{r})$. An incident electric field $\vec{E}^i$ is produced by an external electromagnetic source. Let the scattered electric field be $\vec{E}^s$. Hence the total electric field in the dielectric body is

$$\vec{E} = \vec{E}^i + \vec{E}^s \tag{1}$$

The electric field in the dielectric body can be solved by using the method of induced dielectric current in the dielectric body. Hence the problems becomes that of an induced distributed current source $\vec{J}$ in free space (see *Appendix A*). The induced dielectric current in the dielectric body is related to the electric field by

$$\vec{J} = j\omega\epsilon_o (\epsilon_r - 1) \vec{E} \tag{2}$$

where ω is the angular frequency, ϵ_o is the free space permittivity, and ϵ_r is the complex relative dielectric constant.

Using the induced dielectric current as source, the scattered electric field can be found from

$$\vec{E}^s = -j\omega\vec{A} - \nabla\Phi \tag{3}$$

where

$$\vec{A}(\vec{r}) = \mu_o \iiint_{\text{body}} \frac{\vec{J}(\vec{r}') \exp(-jk_oR)}{4\pi R} dr'^3 \tag{4}$$

$$\Phi(r) = (1/\epsilon_o) \iiint_{\text{body}} \frac{q(\vec{r}') \exp(-jk_oR)}{4\pi R} dr'^3 \tag{5}$$

$$\nabla.\vec{J} = -j\omega q \tag{6}$$

and

$$R = |\vec{r} - \vec{r}'| \tag{7}$$

where $(\vec{r}')$ is the volume charge density and k_o is the free space wave number.

To simplify the notation, an integral operator is defined as follows:

$$\vec{E}^s = -L(\vec{J}) = -j\omega\vec{A} - \nabla\Phi \tag{8}$$

The linear operator L operates on $\vec{J}$ through equation (8). Note that from equation (6), $\nabla.\vec{J}$ is also involved in the operation.

Combining equations (1), (2), and (8), the following equation is obtained:

$$L(\vec{J}) + \vec{J}/j\omega\epsilon_o(\epsilon_r - 1) = E^1 \tag{9}$$

Equation (9) is an integral equation with $E^1(\vec{r})$ as the known function and $\vec{J}(\vec{r})$ as the unknown function.

In order to solve for $\vec{J}(\vec{r})$, a set of basis functions $\{\vec{J}_n\}$ in the domain of L is defined so that

$$\vec{J} = \Sigma\alpha_n\vec{J}_n \tag{10}$$

where α_n are unknown coefficients to be determined. A set of testing functions $\{W_n\}$ in the range of L is also defined.

In order to use Moment Method, the following operation is defined.

$$\langle \vec{J}_{n'}, \vec{W}_n \rangle = \iiint_{\text{body}} \vec{J}_{n'} \cdot \vec{W}_n \, dr'^3 \tag{11}$$

Applying the operation to the testing function $\vec{W}_n$ and equation (9), the following equations are obtained.

$$\sum_{n'=1}^{\infty} \alpha_n \langle \vec{W}_n, \left[L(\vec{J}_n) + \frac{\vec{J}_{n'}}{j\omega\epsilon_0(\epsilon_r - 1)} \right] \rangle = \langle \vec{W}_n, \vec{E}^i \rangle \tag{12}$$

$$n = 1, 2, \ldots \infty.$$

Suppose the function $\vec{J}(\vec{r})$ can be represented by N number of the basis functions. Then, accounting for the three components of the vector $\vec{J}(\vec{r})$, equation (12) is a set of 3N simultaneous equations. Thus the problem is reduced to that of the selection of the basis functions and testing functions and the solution of simultaneous equations.

To apply the Moment Method to the formulation of electromagnetic heating problems in an irregularly-shaped dielectric body simulating part of the human body, the dielectric body is partitioned into N small cells such that each cell has a regular shape and the dielectric property within each cell is uniform. It is worth noting that with this method, various layers of dielectric materials simulating various human tissues are accounted for by the different ϵ's used for different cells. A set of basis functions are defined such that each basis function represents the dielectric current density ($\vec{J}$) in each cell. Thus the problem is to calculate the coefficients α_n in the equation of (12) and to solve the 3N simultaneous equations. The electric field within each cells is obtained from the resultant dielectric current density by using equation (2).

The number of cells needed for accurate calculation depends on the choice of basis functions and testing functions, the variation of dielectric properties in the dielectric body, and the size of the dielectric body compared to wavelength. The choice of simpler basis functions and testing functions require more cells but simplifies the calculations of the coefficients. The greater the variations of the dielectric properties within the body (for example, many layers of tissues), the larger the number of cells are needed. Finally, the larger the body is, compared to wavelength, the larger the number of cells needed.

For most of the practical problems encountered, the theoretical limitations of this method are the proper choice of basis functions and testing functions as was discussed by Harrington [9]. In general, however, for a three-dimensional problem, the number of cells required often are enormous. Thus the computer time and the computer storage requirement might become prohibitively high. Also the problem of accuracy in solving large systems of simultaneous equations might be encountered. In the following section, some calculations are attempted for the plane wave heating in dielectric cylinders with irregular cross sections simulating human limbs.

Plane Wave Induced Dose Pattern in Simulated Human Limbs Using Moment Method

The formulation for plane wave heating in infinitely long dielectric cylinder with irregular cross sections was reported by Richmond for both the E_z (TM) polarization [10] and the H_z (TE) polarization [11]. The Richmond formulation is slightly different from that of Harrington's in that by substituting equation (2)

into equation (9), the electric field becomes the unknown in the simultaneous equations instead of the dielectric current density. For the two-dimensional problem, the cells are circles with radii a_n. For the TM case, the basis functions are pulse functions defined as follows:

$$\vec{E}(x, y) = \sum_{n=1}^{N} E_n(x, y)\,\vec{z} \tag{13}$$

where $E_n(x, y) = E_n$, for $|x - x_n| < a_n/2$, $|y - y_n| < a_n/2$: (14)
$= 0$ otherwise

where E_n is the electric field in the nth cell (x^n, y^n) is the center of the nth cell and $\vec{z}$ is a unit vector along the axial direction of the dielectric cylinder.

The testing functions are impulse functions defined as the following:

$$\vec{W}_n = \delta(x - x_n)\,\delta(y - y_n)\,\vec{z} \tag{15}$$

The following set of simultaneous equations are obtained for the TM case. (See *Appendix B* for detailed derivation).

$$\sum_{n=1}^{N} C_{mn} E_n = E_m^i \qquad m = 1, 2, \ldots N \tag{16}$$

$$C_{mn} = 1 + (\epsilon_m - 1)(j/2)[\pi k_o a_m H_1^{(2)}(k_o a_m) - 2j] \quad \text{for } n = m \tag{17a}$$

$$C_{mn} = (j\pi k_o a_n/2)(\epsilon_n - 1) J_1(k_o a_n) H_o^{(2)}(k_o \rho_{mn}) \quad \text{for } n \neq m \tag{17b}$$

where E_m^i is the incident electric field in the mth cell,
$\rho_{mn} = \{(x_m - x_n)^2 + (y_m - y_n)^2\}^{1/2}$,
(x_n, y_n) is the center of the nth cell, J_1 is the first order Bessel function of the first kind, $H_o^{(2)}$ $H_1^{(2)}$ are the zeroth and first order Hankel functions of the second kind, $k_o = 2\pi/\lambda$, and λ is the wavelength.

The number of cells required for accurate calculation is determined by the criteria

$$2a_n \leq 0.2\lambda/\epsilon_r^{1/2} \tag{18}$$

Table 2 shows the maximum cell sizes $(2a_n)$ that can be used for each tissue layer for the frequency range of 433 MHz to 2450 MHz.

TABLE 2
MAXIMUM CELL SIZE AS A FUNCTION OF FREQUENCY AND TISSUE LAYERS

Frequency MHz	Muscle cell size cm	Fat and Bone cell size cm
433	1.6	5.8
750	1.1	3.4
918	0.9	2.7
2450	0.35	1.0

Calculations are made for the plane wave (TM) induced dose rate pattern of a circular thigh model (Figure 2) using equations (16) and (17). The circular thigh model is partitioned into 130 cells. The cell sizes are less than 2 cm. The dose rate patterns in the circular thigh model are obtained for the 433 MHz case. Using Figure 2, the dose rate pattern in the thigh model obtained from the Moment Method can be compared to the dose rate pattern obtained from the method of summation of cylindrical waves. The results of the two methods agree very well for the region closest to the incident plane wave. However, there is some discrepancy for the regions farther away from the

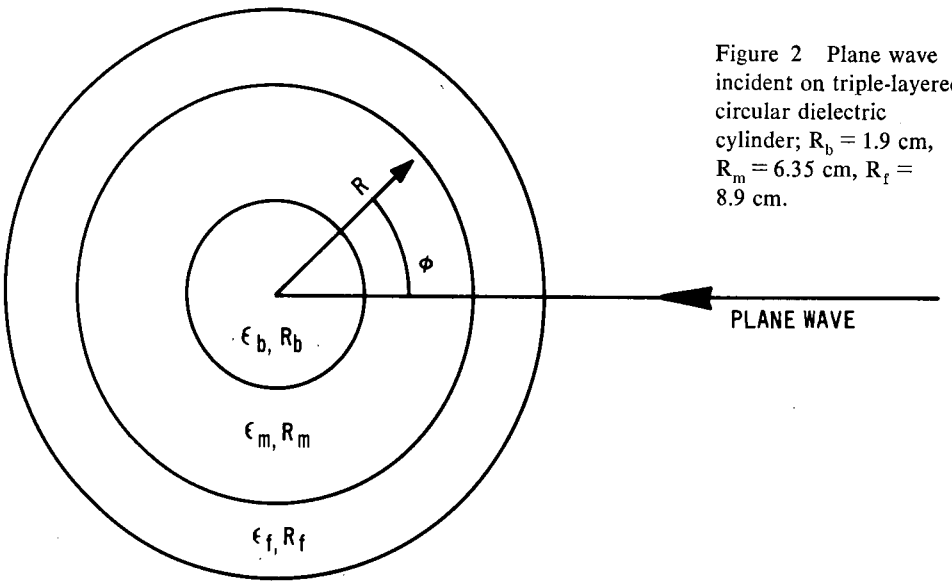

Figure 2 Plane wave incident on triple-layered circular dielectric cylinder; $R_b = 1.9$ cm, $R_m = 6.35$ cm, $R_f = 8.9$ cm.

incident plane wave. The reason for the discrepancy is that more cells (with cell size of 1 cm) are used in the region closest to the incident plane wave while less cells (with cell size of 2 cm) are used in the region away from the incident plane wave. Hence the accuracy in the former region is better than the latter region. Note that in Table 2 the maximum cell size for muscle region at 433 MHz is 1.6 cm. To improve the accuracy, the cross section of the dielectric cylinder must be partitioned into more cells. However, computer time and storage requirement would also increase.

Calculations are also made for the plane wave (TM) induced dose rate pattern of a dielectric cylinder with irregular cross section simulating the size and shape of a human thigh (see Figure 1). The cross section of the thigh model is partitioned into 100 cells. Cell size of 1 cm is used for areas nearest to the incident plane wave. For areas further away from the incident plane wave, cell size of 2 cm is used.

The relative dose rate patterns of the 750 MHz and 433 MHz cases are shown in Figures 3 and 4. For both cases, the regions of maximum dose rate are at the two corners of the model in the muscle region.

Experimental results of the cross-sectional temperature patterns of the irregular phantom thigh model due to aperture sources for the cases of 433 MHz, 750 MHz, 918 MHz and 2450 MHz has been reported by Guy [12]. However, comparison between the data in the present investigation and the experimental data is difficult due to the different sources used in the two investigations.

Three Dimensional Irregular Dielectric Bodies

The calculations for the dose rate patterns in an irregular dielectric body (such as the model for a part of the human body) due to arbitrary external electromagnetic sources (with $\vec{E}^i$ defined) are very complicated and may require enormous amount of computer time. Although the Moment Method can be utilized for the solution of the problem, care must be taken in the selection

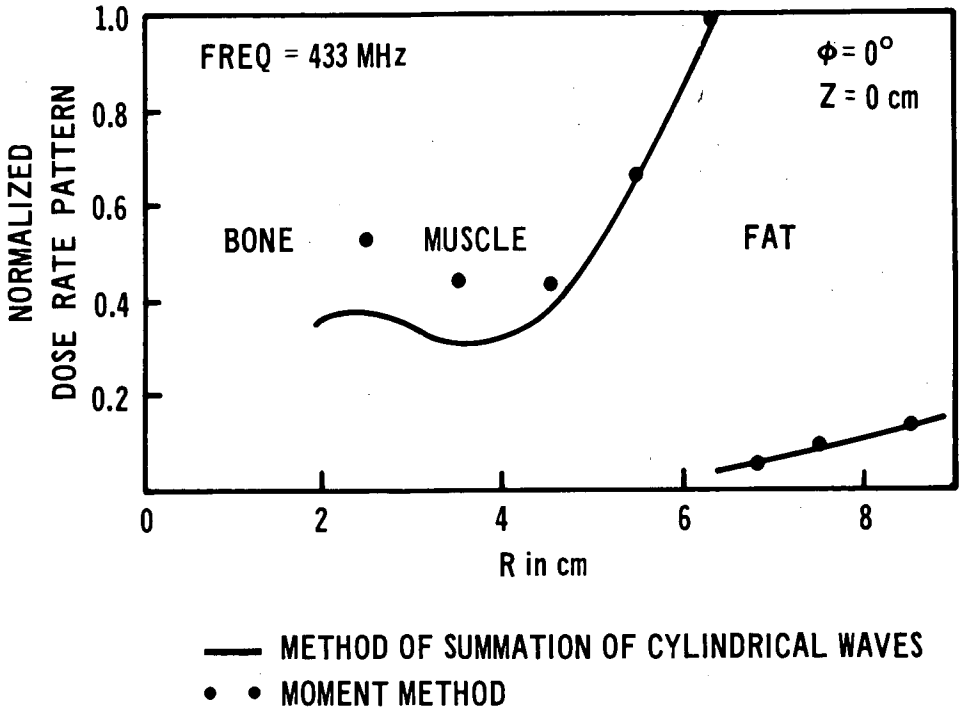

Figure 3 Dose rate pattern in circular thigh model irradiated by an incident plane wave normally incident on the cylinder and with TM polarization.

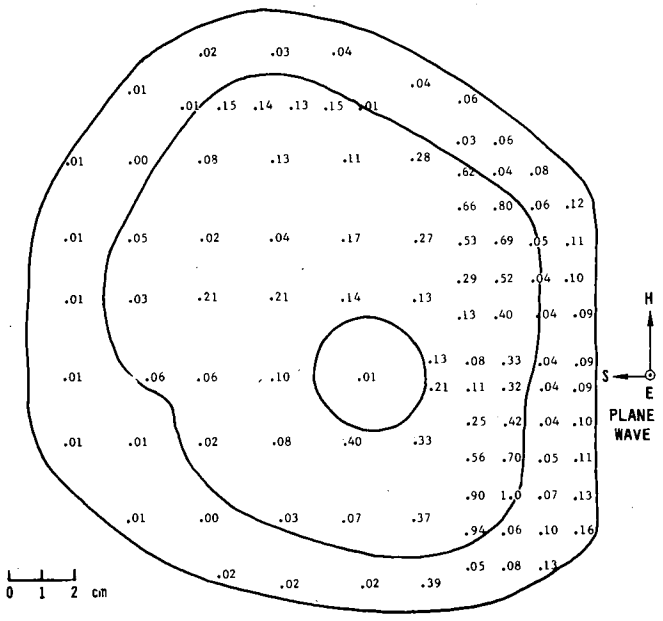

Figure 4 Normalized dose rate pattern in irregular thigh model irradiated by a 750 MHz plane wave normally incident on the cylinder and with TM polarization.

of the basis functions and the testing functions. Considerations also must be given to the difficulty and the amount of time required for the solution of the integrals encountered during the calculations for the coefficients of the simultaneous equations in equation (12). Accuracy for the solution of the simultaneous equations when the number of equations are large is yet another problem.

In spite of the problems mentioned, a brief discussion of an approach for solving the three dimensional problem using Moment Method is presented. Consider the irregular dielectric body previously discussed. Consider also the incident electric field $\vec{E}^i$ which is defined. Following the previous formulation, the induced dielectric current (and hence the total electric field) in the dielectric body can be obtained by solving the simultaneous equations in equation (12). The problem hence is to partition the dielectric body into N cells and to select a set of N number of basis functions and a set of N number of testing functions. Partitioning the dielectric body into cubic cells which have the same size, let each side of the cells have the dimension of a.

A set of triangular functions is selected as the basis functions. The dielectric current density $\vec{J}$ is therefore represented as:

$$\vec{J} = \sum_{n'=1}^{N} [J_{n'}{}^{x} T_{n'}(x', y', z')\,\vec{x} + J_{n'}{}^{y} T_{n'}(x', y', z')\,\vec{y} + J_{n'}{}^{z} T_{n'}(x', y', z')\,\vec{z}] \tag{19}$$

where

$$T_{n'}(x', y', z') = 8/a^3\,[(a/2 - |x' - x_{n'}|)\,(a/2 - |y' - y_{n'}|)\,(a/2 - |z' - z_{n'}|)] \tag{20a}$$

$$\text{for } |x' - x_{n'}| < a/2,\ |y' - y_{n'}| < a/2, \text{ and } |z' - z_{n'}| < a/2. \tag{20b}$$

$$T_{n'}(x', y', z') = 0 \text{ otherwise}$$

where $(x_{n'}, y_{n'}, z_{n'})$ is the center of the n'th cell.

Let the set of testing functions be impulse functions:

$$\vec{W}_n = [\delta(x - x_n)\,\delta(y - y_n)\,\delta(z - z_n)]\,[\vec{x} + \vec{y} + \vec{z}] \tag{21}$$

where (x_n, y_n, z_n) is the center of the nth cell.

Substituting the set of basis functions and the set of testing functions into equation (12), the following set of simultaneous equations are obtained.

$$\sum_{n'=1}^{N} [-j\omega\mu_o J_{n'}{}^{x} \Phi(x_n, y_n, z_n; x_{n'}, y_{n'}, z_{n'}) + \{1/j\omega\epsilon_o (\epsilon_r - 1)\} J_{n'}{}^{x} - (1/j\omega\epsilon_o)(\partial/\partial x)\,\Psi(x, y, z; x_{n'}, y_{n'}, z_{n'})\,|_{(x_n, y_n, z_n)}]$$

$$= E_n{}^{ix}(x_n, y_n, z_n) \tag{22}$$

$$\sum_{n'=1}^{N} [-j\omega\mu_o J_{n'}{}^{y} \Phi(x_n, y_n, z_n; x_{n'}, y_{n'}, z_{n'}) + \{1/j\omega\epsilon_o (\epsilon_r - 1)\} J_{n'}{}^{y} - (1/j\omega\epsilon_o)(\partial/\partial y)\,\Psi(x, y, z; x_{n'}, y_{n'}, z_{n'})\,|_{(x_n, y_n, z_n)}]$$

$$= E_n{}^{iy}(x_n, y_n, z_n) \tag{23}$$

$$\sum_{n'=1}^{N} [-j\omega\mu_o J_{n'}{}^{z} \Phi(x_n, y_n, z_n; x_{n'}, y_{n'}, z_{n'}) + \{1/j\omega\epsilon_o (\epsilon_r - 1)\} J_{n'}{}^{z} - (1/j\omega\epsilon_o)(\partial/\partial z)\,\Psi(x, y, z; x_{n'}, y_{n'}, z_{n'})\,|_{(x_n, y_n, z_n)}]$$

$$= E_n{}^{iz}(x_n, y_n, z_n) \tag{24}$$

$n = 1, 2, 3, \ldots N$, $\epsilon_r = \epsilon_{n'}$ = dielectric constant in n'th cell

where

$$\Phi(x_n, y_n, z_n; x_{n'}, y_{n'}, z_{n'}) = \sum_{n'}^{\text{cell}} \iiint \frac{T_{n'}(x', y', z') \exp(-jk_o |\vec{r}_n - \vec{r}'|)}{4\pi |\vec{r} - \vec{r}'|} dr'^3 \tag{25}$$

$$\Psi(x, y, z; x_{n'}, y_{n'}, z_{n'}) = \sum_{\text{cell}} \iiint [J_{n'}{}^x \partial T_{n'}/\partial x' + J_{n'}{}^y \partial T_{n'}/\partial y' + J_{n'}{}^z \partial T_{n'}/\partial z')] \times \frac{\exp(-jk_o |\vec{r} - \vec{r}'|)}{4\pi |\vec{r} - \vec{r}'|} dr'^3 \tag{26}$$

and

$$|\vec{r}_n - \vec{r}'| = \sqrt{(x_n - x')^2 + (y_n - y')^2 + (z_n - z')^2} \tag{27}$$

$$|\vec{r} - \vec{r}'| = \sqrt{(x - x')^2 + (y - y')^2 + (z - z')^2} \tag{28}$$

Hence the values of Φ, $\partial\Psi/\partial x$, $\partial\Psi/\partial y$, and $\partial\Psi/\partial z$ have to be solved. Substituting the expressions for T_n, into equations (25) and (26), the following equations are obtained.

$$\Phi(x_n, y_n, z_n; x_{n'}, y_{n'}, z_{n'}) = 8/a^3 \left[\int_{-a/2 + z_{n'}}^{a/2 + z_{n'}} \int_{-a/2 + y_{n'}}^{a/2 + y_{n'}} \int_{-a/2 + x_{n'}}^{a/2 + x_{n'}} \{(a/2 - |x' - x_{n'}|)(a/2 - |y' - y_{n'}|)(a/2 - |z' - z_{n'}|) \times \frac{\exp[-jk_o \sqrt{(x_n - x')^2 + (y_n - y')^2 + (z_n - z')^2}]}{4\pi \sqrt{(x_n - x')^2 + (y_n - y')^2 + (z_n - z')^2}} \} dx'dy'dz' \right] \tag{29}$$

$$\frac{\partial \Psi}{\partial x}(x, y, z; x_{n'}, y_{n'}, z_{n'}) = \int_{-a/2 + z_{n'}}^{a/2 + z_{n'}} \int_{-a/2 + y_{n'}}^{a/2 + y_{n'}} \int_{-a/2 + x_{n'}}^{a/2 + x_{n'}} [G(x', y', z') H_x(x, y, z; x', y', z')] dx'dy'dz' \tag{30}$$

where

$$G(x', y', z') = J_{n'}{}^x \partial T_{n'}/\partial x' + J_{n'}{}^y \partial T_{n'}/\partial y' + J_{n'}{}^z \partial T_{n'}/\partial z' \tag{31}$$

$$\partial T_{n'}/\partial x' = 8/a^3 (a/2 - |y' - y_{n'}|)(a/2 - |z' - z_{n'}|) \quad \text{for } |x' - x_{n'}| \leq a/2 \tag{32}$$

$$= -8/a^3 (a/2 - |y' - y_{n'}|)(a/2 - |z' - z_{n'}|) \quad \text{for } |x' - x_{n'}| > a/2$$

$$\partial T_{n'}/\partial y' = 8/a^3 (a/2 - |x' - x_{n'}|)(a'2 - |z' - z_{n'}|) \quad \text{for } |y' - y_{n'}| \leq a/2$$

$$= -8/a^3 (a/2) - |x' - x_{n'}|)(a/2 - |z' - z_{n'}|) \quad \text{for } |y' - y_{n'}| > a/2 \tag{33}$$

$$\partial T_{n'}/\partial z' = 8/a^3 (a/2 - |x' - x_{n'}|)(a/2 - |y' - y_{n'}|) \quad \text{for } |z' - z_{n'}| \leq a/2 \tag{34}$$

$$= -8/a^3 (a/2 - |x' - x_{n'}|)(a/2 - |y' - y_{n'}|) \quad \text{for } |z' - z_{n'}| > a/2$$

and

$$H_x(x, y, z; x', y', z') = \frac{-jk_o (x - x') \exp(-jk_o |\vec{r} - \vec{r}'|)}{4\pi |\vec{r} - \vec{r}'|^2} - \frac{(x - x') \exp(-jk_o |\vec{r} - \vec{r}'|)}{4\pi |\vec{r} - \vec{r}'|^{3/2}} \tag{35}$$

where $|r - r'|$ is defined in equation (28).

The expressions for $\partial\Psi/\partial y$ and $\partial\Psi/\partial z$ can be obtained in the same manner as that for $\partial\Psi/\partial x$. The integrals in the equations (29) and (30) are difficult to solve in closed form and may require numerical integration for their solutions. Thus the problem encountered is that of enormous computation time. For example, if the irregularly-shaped body is divided into 1000 cells, the number of simultaneous equations are 3000. The number of coefficients in the equations are 9 million. Hence 9 million numerical integrations in three dimensions are required. The solution for numerical results in the three dimensional problem is therefore beyond the scope of this investigation.

Conclusion

Further research on the heating patterns in three dimensional irregularly-shaped dielectric models of human tissues is needed. Although, in principle, the Moment Method should give the field distribution in the three-dimensional case, in practice, the large amount of calculation required presents serious difficulties. More research can be directed towards minimizing the computation time by judicious selection of basis functions and testing functions.

Acknowledgements

The content of this paper is part of the author's Ph.D. dissertation performed at the Electrical Engineering Department and the Department of Rehabilitation Medicine, University of Washington, Seattle, Washington. The author gratefully acknowledges the help and advice of Professors R. A. Sigelmann and A. W. Guy of the University of Washington during the performance of this work. The author also wishes to acknowledge the financial support of Social and Rehabilitation Service Grant RT-3, University of Washington Initiative 171 Funds, the Bioengineering Program Project, National Institute of Health Grant GM 16436-01, and the Bureau of Radiological Health Grant 8-R01-RL00528-02.

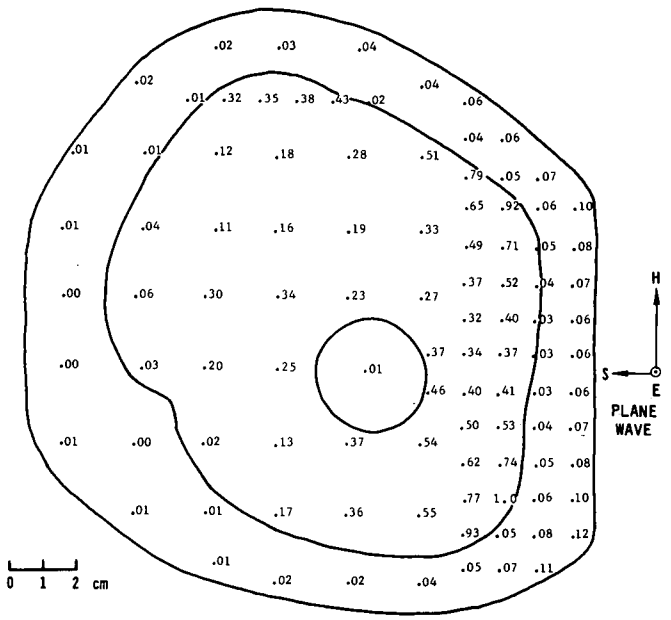

Figure 5 Normalized dose rate pattern in irregular thigh model irradiated by a 433 MHz plane wave normally incident on the cylinder and with TM polarization.

References

1 Anne, A., Saito, M., Salati, O. M. and Schwan, H. P., "Relative microwave absorption cross sections of biological significance," *Biological Effects of Microwave Radiation, 1,* Plenum Press, pp. 153-177, 1960.

2 Johnson, C. C. and Guy, A. W., "Nonionizing electromagnetic wave effects in biological materials and systems," Proc. IEEE, *60,* pp. 692-718, 1972.

3 Guy, A. W., "Electromagnetic fields and relative heating patterns due to a rectangular aperture source in direct contact with bilayered biological tissues," IEEE Trans. M.T.T., *MTT-19,* pp. 214-223, Feb. 1971.

4 Ho, H. S., Guy, A. W., Sigelmann, R. A. and Lehmann, J. F., "Microwave heating of simulated human limbs by aperture sources," IEEE Trans. M.T.T., *MTT-19,* pp. 224-231, Feb. 1971.

5 Shapiro, A. R., Lutomirski, R. F. and Yura, H. T., "Induced fields and heating within a cranial structure irradiated by an electromagnetic plane wave," IEEE Trans. M.T.T., *MTT-19,* pp. 187-196.

6 Ho, H. S., "Contrast of dose distribution in phantom heads due to aperture and plane wave sources," Annals of the New York Academy of Science, 1974.

7 Schwan, H. P. and Piersol, G. M., "The absorption of electromagnetic energy in body tissues," Amer. J. Phys. Med., *33,* pp. 370-404, Dec. 1954.

8 Yee, H. Y., "Scattering of electromagnetic waves by circular dielectric coated conducting cylinders with arbitrary cross sections," IEEE Trans. A.P., *AP-13*(5), pp. 822-823, Sept. 1965.

9 Harrington, R. F., *Field Computation by Moment Methods,* MacMillan Co., New York, 1968.

10 Richmond, J. H., "Scattering by a dielectric cylinder of arbitrary cross-section shape," IEEE Trans. A.P. *AP-13,* pp. 334-341, May 1965.

11 Richmond, J. H., "TE-Wave scattering by a dielectric cylinder of arbitrary cross-section shape," IEEE Trans. A.P., *AP-14*(4), pp. 460-464, July 1966.

12 Guy, A. W., "Analyses of electromagnetic fields induced in biological tissues by thermographic studies on equivalent phantom models," IEEE Trans. M.T.T., *MTT-19,* pp. 205-213.

Appendix A
Derivation of Equation (2)

Consider the fields in a dielectric body due to external sources. Within the dielectric body, there is no physical source. Hence the Maxwell's equations are

$$\nabla \times \vec{H} = j\omega\epsilon_r\epsilon_o \vec{E} \tag{1A}$$

$$\nabla \times \vec{E} = -j\omega\mu_o \vec{H} \tag{2A}$$

Rearranging equation (1A)

$$\nabla \times \vec{H} = j\omega\epsilon_o \vec{E} + j\omega\epsilon_o (\epsilon_r - 1) \vec{E} \tag{3A}$$

Now define the following

$$\vec{J} = j\omega\epsilon_o (\epsilon_r - 1) \vec{E} \tag{4A}$$

In this case $\vec{J}$ is an induced dielectric current source. Thus the set of Maxwell's equations becomes

$$\nabla \times \vec{H} = j\omega\epsilon_o \vec{E} + \vec{J} \tag{5A}$$

$$\nabla \times \vec{E} = -j\omega\mu_o \vec{H} \tag{6A}$$

Hence, the problem becomes that of an induced distributed current source $\vec{J}$ in free space.

Appendix B
Derivation of Equations (16) and (17)

Consider the two dimensional problem of an E_z polarized (TM) plane wave normally incident on a dielectric cylinder with irregular cross section. The incident electric field is along the z direction.

$$\vec{E}^i = E^i(x, y)\,\vec{z} \tag{1B}$$

A scattered electric field, also in the z direction is induced by the incident field.

$$\vec{E}^s = E^s(x, y,)\,\vec{z} \tag{2B}$$

Thus the total electric field in the dielectric cylinder is along the z axis.

$$\vec{E}\,z = (E^i + E^s)\,\vec{z} \tag{3B}$$

From equation (4.2) the induced dielectric current is

$$J\vec{z} = j\omega\epsilon_o(\epsilon_r - 1)\,E\vec{z} \tag{4B}$$

The electric field generated by an increment of current dI parallel to the z axis is given by

$$d\vec{E}^s = -\vec{z}\,(\omega\mu_o/4)\,H_o^{(2)}(k_o\rho)\,dI \tag{5B}$$

where $H_o^{(2)}(k_o\rho)$ is Hankel function the second kind of order zero. $k_o = 2\pi/\lambda$ is the free space wave number.

$$\rho^2 = (x - x')^2 + (y - y')^2$$

where (x, y) is the field point and (x', y') is the source point. Putting $dI\,\vec{z}$ in terms of $\vec{J}$,

$$dI\,\vec{z} = J\,ds\,\vec{z} = j\omega(\epsilon_r - 1)\epsilon_o\,E\,\vec{z} \tag{6B}$$

Combining equations (5B) and (6B),

$$E^s(x, y) = -(jk_o^2/4)\iint \{\epsilon_r(x', y') - 1\}\,E(x', y')\,H_o^{(2)}(k_o\rho)\,dx'dy' \tag{7B}$$

$$E(x, y) + (jk_o^2/4)\iint (\epsilon_r - 1)\,E(x', y')\,H_o^{(2)}(k_o\rho)\,dx'dy' = E^i(x, y) \tag{8B}$$

The cross section of the dielectric cylinder is divided into N number of small cells so that within each cell, the dielectric constant and the electric field are almost constant. Thus equation (8B) holds true at the center of each cell. Considering equation (8B) at the center of the mth cell,

$$E_m + (jk_o^2/4)\sum_{n=1}^{N}(\epsilon_n - 1)\,E_n \iint_{\text{cell } n} H_o^{(2)}(k_o\rho)\,dx'dy' = E_m^i \tag{9B}$$

$$m = 1, 2, \ldots N$$

where E_n is the electric field in cell n, and ϵ_n is the complex dielectric constant of cell n.

$$\rho^2 = (x' - x_m)^2 + (y' - y_m)^2 \tag{10B}$$

To solve for the values of the integrals in equation (9B), consider the cells to be circles with radius a_n for the nth cell. The integrals can be solved in closed form as follows:

$$(jk_o^2/4)\int_0^{2\pi}\int_0^{a_n} H_o^{(2)}(k_o\rho)\,\rho'd\rho'd\Phi'$$

$$= (j/2)\,[\pi k_o a_m H_1^{(2)}(k_o a_m) - 2j] \qquad \text{if } m = n \tag{11B}$$

$$= (j\pi k_o a_n/2)\,J_1(k_o a_n)\,H_o^{(2)}(k_o\rho_{mn}) \qquad \text{if } m \neq n \tag{12B}$$

where

$$\rho_{mn}^2 = (x_m - x_n)^2 + (y_m - y_n)^2 \tag{13B}$$

Hence the system of linear equations can be written in the following form:

$$\sum_{n=1}^{N} C_{mn}\,E_n = E_m^i \qquad m = 1, 2, \ldots N \tag{14B}$$

$$C_{mn} = 1 + (\epsilon_m - 1)\,(j/2)\,[k_o a_m H_1^{(2)}(k_o a_m) - 2j] \qquad \text{if } n = m \tag{15B}$$

$$C_{mn} = (j\pi k_o a_n/2)\,(\epsilon_n - 1)\,J_1(k_o a_n)\,H_o^{(2)}(k_o\rho_{mn}) \qquad \text{if } n \neq m \tag{16B}$$

Equations (14B), (15B), and (16B) are the same as equations (16) and (17).